Characterization of CuO thin films for gas sensing applications

Jamal M. Rzaij

Department of Physics, College of Science, Al Anbar University, Iraq

E-mail: jam72al@yahoo.com

Abstract

Nanostructural cupric oxide (CuO) films were prepared on Si and glass substrate by pulsed laser deposition technique (PLD) using laser Nd:YAG, using different laser pulses energies from 200 to 600 mJ. The X-ray diffraction pattern (XRD) of the films showed a polycrystalline structure with a monoclinic symmetry and preferred orientation toward (111) plane with nano structure. The crystallite size was increasing with increasing of laser pulse energy. Optical properties was characterized by using UV–vis spectrometer in the wave lengthrange (200-1100) nm at room temperature. The results showed that the transmission spectrum decreases with the laser pulses energy increase. Sensitivity of NO_2 gas at different operating temperatures, (50°C, 100°C, 150°C and 200°C) was calculated.

Key words

Copper oxide, thin films, structural properties, NO_2 gas.

Article info.

Received: Mar. 2016
Accepted: Apr. 2016
Published: Dec. 2016

وصف أغشية اوكسيد النحاس الرقيقة لتطبيقات التحسس الغازي

جمال مال الله رزيج

قسم الفيزياء، كلية العلوم، جامعة الانبار، العراق

الخلاصة

تحضير اغشية اوكسيد النحاس النانوية على ارضيات من الزجاج والسليكون باستخدام تقنية الترسيب بالليزر النبضي باستخدام ليزر النيدميوم –ياك باستخدام طاقات نبضة ليزر مختلفة من 200 الى 600 ملي جول. ان نمط حيود الاشعة السينية اظهرت أن الأغشية تمتلك تركيب متعدد البلورات ذات تناظر من النوع احادي الميل بدورانية (111) وذات تركيب نانوي. كانت هناك زيادة في الحجم الحبيبي مع زيادة طاقة نبضة الليزر. تم تمييز الخصائص البصرية باستخدام مطياف الاشعة فوق البنفسجية-المرئية ضمن مدى الطول الموجي (200 الى 1100 نانومتر) بدرجة حرارة الغرفة، أظهرت النتائج ان طيف النفاذية يقل مع زيادة طاقة نبضة الليزر. تم حساب التحسسية لغاز ثاني اوكسيد النتروجين (NO_2) عند درجات حرارية مختلفة (50 °م، 100°م، 150 °م و 200 °م).

Introduction

Transparent conducting oxides (TCOs) are electrical conductive materials with a comparably low absorption of light, they are usually prepared with thin film technologies[1]. In recent years, nanostructures of transparent metal oxides have gained a great attention from material scientists and engineers due to their different properties compared with the corresponding bulk counterparts, which in turn provides promising applications in various fields of technology [2]. Among metal oxide, CuO is attractive materials and many studies on copper oxide nanomaterial have grown substantially due to its direct band gap (1.2-2.0 eV)[3], and intrinsic p-type behavior together with good electrochemical properties and low cost fabrication. There two most important types of polymorphism in the CuO compounds: cuprous oxide (Cu_2O) and cupric oxide (CuO) [4]. Oxide semiconductors have been used to detect oxidizing and reducing gases in a simple and cost-effective manner [5]. Their chemiresistive variation emanates from

the oxidative or reductive interaction of the analytic gas with the oxide semiconductor surface and the consequent change in the charge carrier concentration. In n-type oxide semiconductor gas sensors such as those comprising SnO_2, ZnO, TiO_2, WO_3 and In_2O_3, the electron depletion layer is formed by the adsorption of negatively charged oxygen, which dominates the overall conduction process [6]. In contrast, for p-type oxide semiconductor gas sensors such as those comprising CuO, NiO, Co_3O_4 and Cr_2O_3, the adsorption of negatively charged oxygen forms a hole accumulation layer near the surface. Thus, conduction occurs along the conductive hole accumulation layer[7]. Many technique were used to grow CuO thin films including: spray pyrolysis by (J. Morales et al.) [8], pulsed laser deposition (PLD) by (Y. R. Hathal et al.) [9], chemical vapor deposition (CVD) by (Maruyama)[10], sol-gel by (N. Nafarizal) [11], thermal oxidation by (Shanid & Khadar 2008) [12] and the reactive sputtering by (Ogwu et al.) [13].

Aim of the work

This Work Report the effect of laser pulse energy increasing on structural and optical properties of CdO thin films and processing gas sensor device for nitrogen dioxide (NO_2) gas.

Experemental procedure

CuO with high purity of 99.999 % is pressed under pressure of 5 ton to form a target of 1.5 cm diameter and 0.2 cm thickness. Thin films of CuO are deposited on glass and n-type Si substrates with orientation (111) utilizing pulsed laser deposition technique at room temperature with thickness about of 100 nm using depth profile probe (TF probe) model SR300 (Angstrom Sun Technologies Inc., USA) with a wavelength range from 200 to 1100 nm. The X-ray diffraction (XRD) spectra of the films were obtained to verify their crystal structure using instrument model (Cu-Kα) radiation with $\lambda = 0.154$ nm. Optical transmission data were obtained using UV-vis double beam spectrometer at wavelengths ranging from 200 nm to 1100 nm.

Results and discussion

Structural properties

Fig.1 represents the x-ray diffraction of the CuO thin films at different laser pulse energy (200, 300, 400, 500 and 600) mJ. The films are polycrystalline structure with a monoclinic symmetry and lattice constant of: a=4.6700 Å, b=3.4300 Å, c=5.1200 Å and β=99.530º according to the (JCPDS No. 96-101-1195). The high intensity and sharp peak at 2θ=28° attributed to the crystalline Si substrate with crystalline plane (111). For 200 mJ pulse energy, XRD patterns possess many diffraction peaks which indicate the formation of polycrystalline CuO with planes (110), (11-1) and (111). At 300 mJ pulse energy there was increasing in the intensities of diffraction peaks and appearance of new diffraction peaks (020) located at 2θ=53.4° with a weak intensity, while at 400 mJ pulse energy many additional peaks are appearance with maximum intensity (253 arbitrary unit) which is attributable to the Drift competitive growth model which is called (the model of the survival of the fastest growing crystallites). Drift was assumed that the process of Nucleation takes several directions in the early stages from the growth of the films and then begin to compete during growth and the fastest-nuclei continue to grow while the other nucleus stops from growth [28].

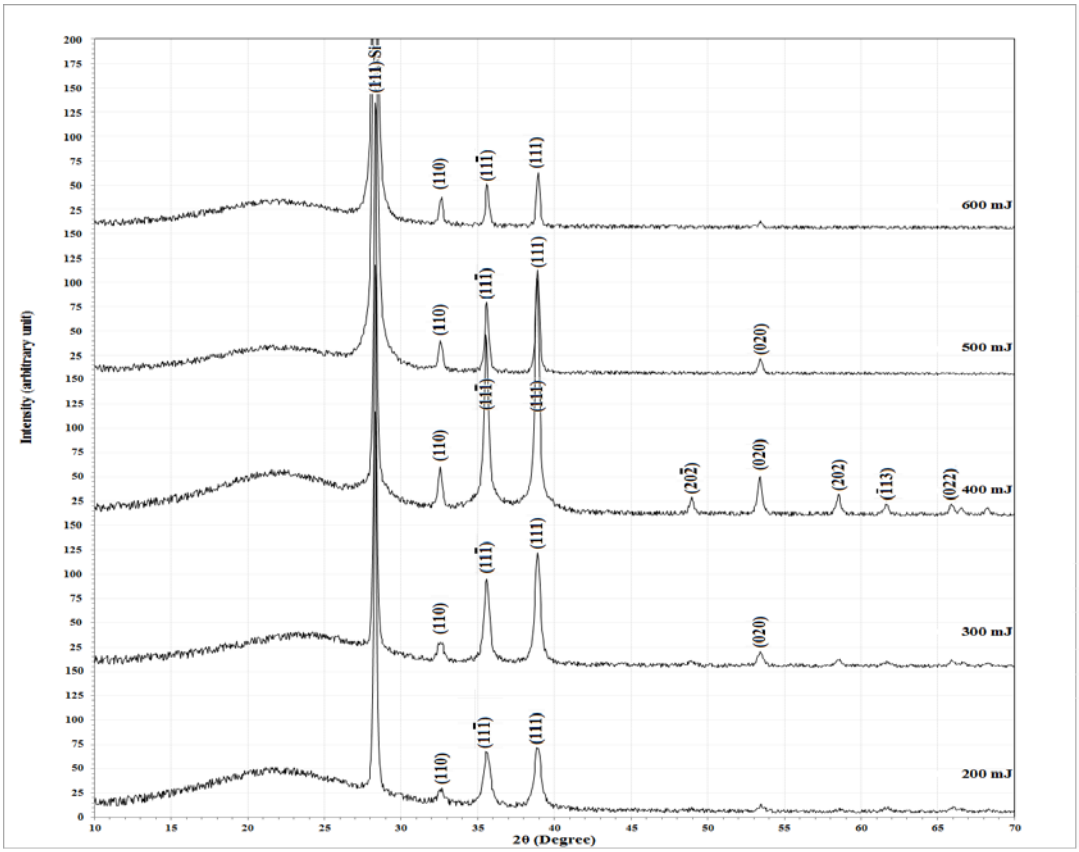

Fig.1: X-ray diffraction pattern of copper oxide thin film.

Decrease in the FWHM of the (111) peak of CuO indicates the enhancement in the crystallite sizes of CuO with the increasing in the laser pulse energy. a well crystalline spectrum at 400 mJ can be attributed to an improvement in the crystalline structure and formation of a new nucleating centers resulting from the decrease of nucleation energy barrier[14], thus, the highly crystalline peak grown at 400 mJ pulse energy show FWHM of 0.3144°, while for 500 and 600 mJ pulse laser energies there was decreasing in the intensities of diffraction peaks attributed to the saturation of new nuclei [15]. The presents a preferential orientation of the film was along the plane (111) at diffraction angle of 2θ =38.92°, d =2.31 nm.

The average crystallite size (D) of crystal CuO was determined from the spectrum of X-ray taking into account full width at half maximum (FWHM), which is given by Scherer's formula: [16]

$$D = \frac{k\lambda}{\beta \cos(\theta)} \qquad (1)$$

where k: is the shape factor, β:is the full width at half maximum (FWHM) in radian, λ: is the X-ray wavelength and θ: is Bragg's which represents the incident angle. There was increasing in crystallite size with increasing laser pulse energy as a result to an increasing in the numbers of ejected particles from CuO target toward substrate, as shown in Fig. 2.

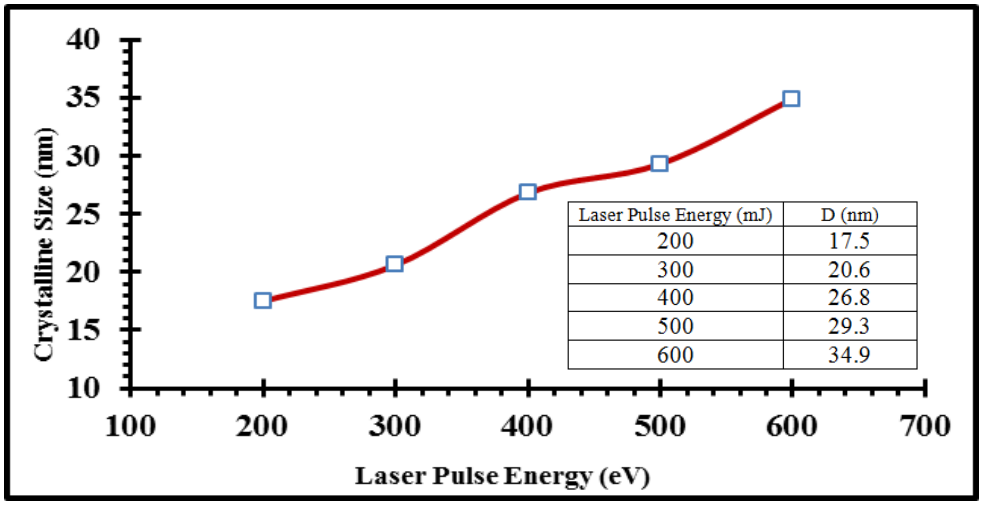

Laser Pulse Energy (mJ)	D (nm)
200	17.5
300	20.6
400	26.8
500	29.3
600	34.9

Fig. 2: The variation of crystallite size as a function to the laser pulse energy.

Optical properties

Transmittance (T)

Fig.3 shows the transmittance spectra of CuO thin films in the range (200-1100) nm which are deposited on glass substrates with variation of crystallite size at room temperature, which calculated from the relation:

$$T = e^{-2.303\,A} \quad (2)$$

where T is the transmittance and A is the absorbance.

The rapid increase in transmittance of prepared samples with increasing of wavelength within the range of 300-550 nm, then linear increase in transmittance after a wavelength of 550 nm, which then can be concluded absorption edge.

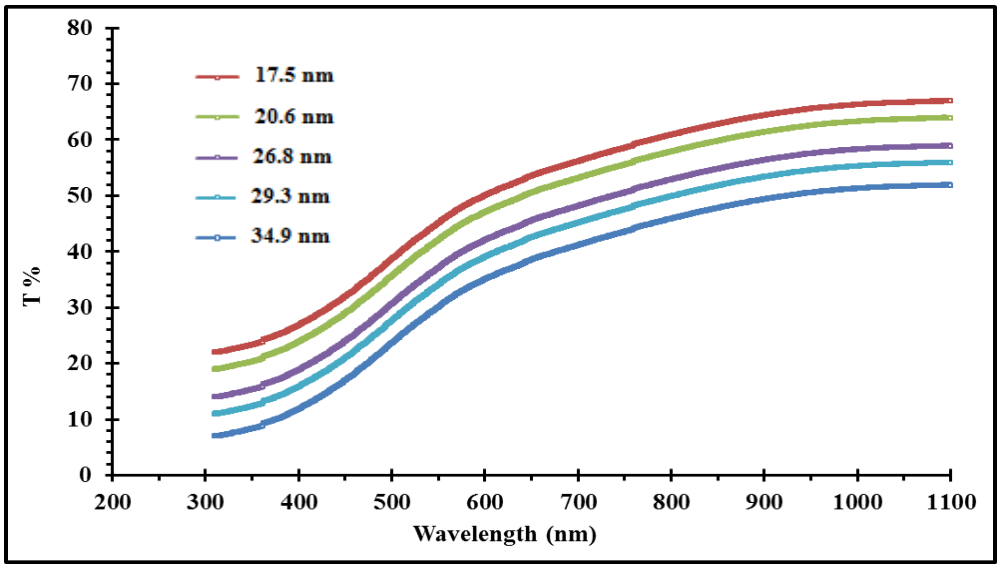

Fig. 3: Transmittance as a function of wavelength.

The rapid increase in transmittance can be attributed to the occurrence of the electrons transitions in energy levels within the bands (Intraband Transitions), while decreasing in transmittance with increasing the incident laser energy reveal to an increase in the numbers of ejected particles from CuO target toward the substrate as a result to increasing in the energies of incident pulses laser. When the pulses of laser incident towards the

target, the ejected particles will have high kinetic energy which absorb this energy from incident laser pulse leads to increasing in the film thickness then decreasing in transmittance of films. The maximum transmittance was 64% in the wavelength spectrum of 900 nm for film of 200 mJ pulses energy, while the minimum transmittance was 48% in the wavelength spectrum of 900 nm for film of 600 mJ pulses energy.

Absorption coefficient (α)

The variation of absorption coefficient (α) for CuO film as a function to the wavelength is shown in Fig.4, which calculated from the relation: [3]

$$\alpha = 2.303\frac{A}{t} \qquad (3)$$

where A is the absorbance and t is the thickness of film.

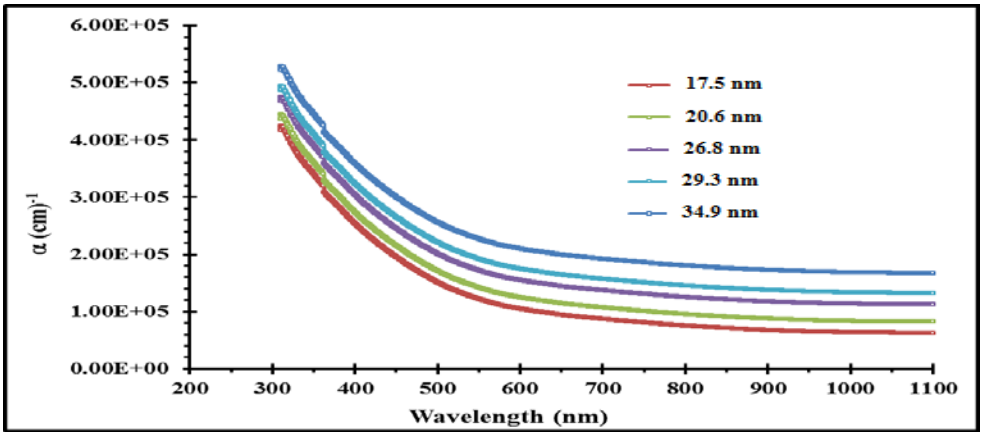

Fig. 4: Absorption coefficient as a function of wavelength.

The absorption coefficient spectra reveal that films grown under the same parametric conditions have a low absorbance in the visible / near infrared region. In the end of ultraviolet region, (α) exhibits high values, (larger than 10^4 cm^{-1}), which means that there is a large probability of the allowed direct transition. In the region of 300-550 nm, the absorption coefficient (α) takes values larger than 2×10^5 cm^{-1} and then decreases with increasing wavelength and in the range of 550-1100 nm the regression becomes simple which is attributable to the relative stability of the rate of increase in transmittance within this spectral region where the absorption coefficient has small values at high wavelengths, depending on the opposite relation between transmittance and absorption coefficient. It is revealed that the absorption coefficient has opposite behavior as compared to the transmittance. In other words, it is increase with increasing of crystallite size may be due to creating of localized states in the energy gap [17].

Optical energy gap (E_g)

A direct optical energy gap, according to high values of absorption coefficient (α ≥10^4 cm^{-1}) [18], for CuO films deposited on glass substrate at room temperature was calculated using Tauc equation [19]:

$$(\alpha h\nu)^2 = B(h\nu - E_g) \qquad (4)$$

where h: is the plank constant, ν is the frequency of incident photon, α: is the absorption coefficient, hν: is the energy of incident photon, B is a constant and E_g is the optical energy gap.

The plot of $(\alpha h\gamma)^2$ as a function to the photon energy is shown in Fig. 5.

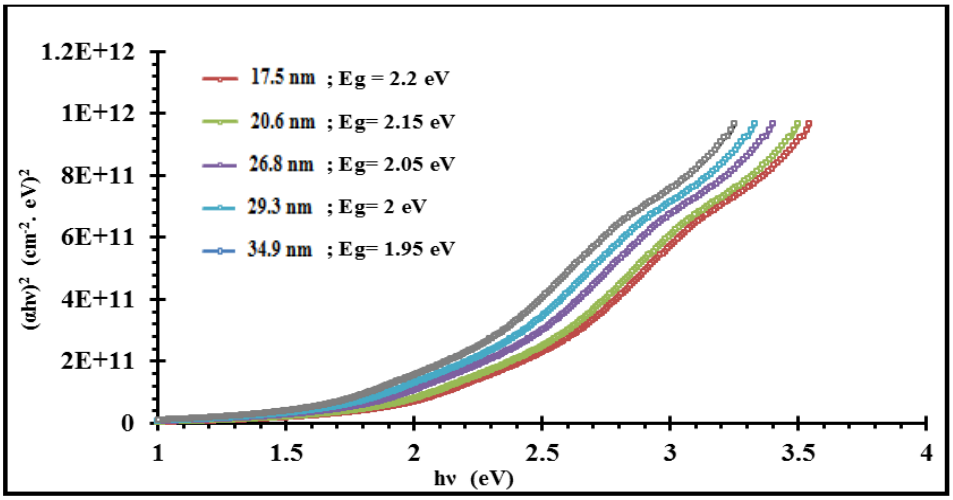

Fig. 5: Tauc plot for CuO film at variation crystallite size.

The point of intersection between the straight line and the axis of the photon energy gives the optical energy band gap. It can be observed that (E_g) is decreasing slightly into lower energies or longer wavelengths region (redshift), as shown in Fig. 6.

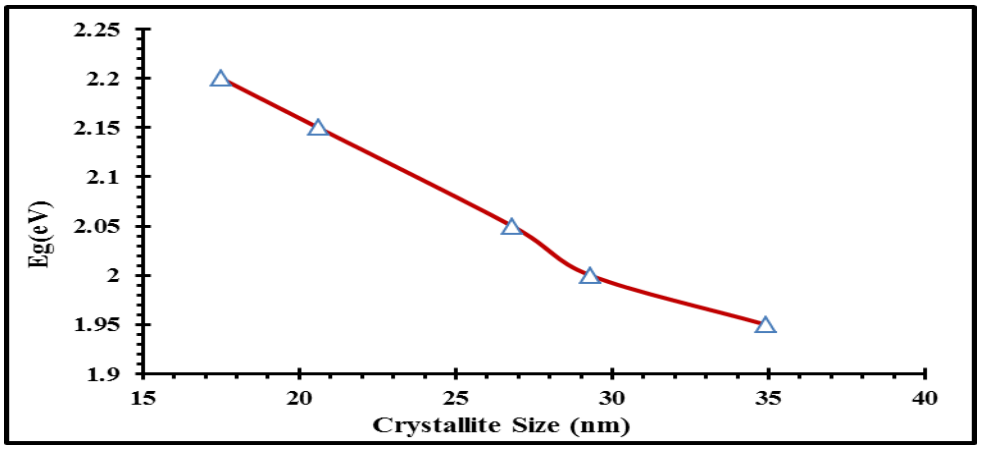

Fig. 6: Variation of E_g with variation of crystallite size.

The linear decrease in energy gap with the increase in crystallite size is because of the high laser pulse energy giving a high kinetic energy to the ablated atoms from Cu target then the absorbance of atoms will increase because of formation of localize state within the energy gap and near the conductive band which has worked in turn displaces Fermi level toward conductive band then absorb the photons which have energy less than that of energy gap, hence, the energy gap decreases according to the Eq. (4) as the laser energy pulse increases.

Gas sensing measurement sensing behavior of NO_2

The sensing properties of CuO films deposit on silicon substrate for NO_2 gas sensing are investigated as a function of operation temperature and time with concentration of about 10 ppm at different operation temperature (RT, 100, 150 and 200) °C. Fig.7 show the variation of CuO resistance as a function of time for both cases open and closed gas with variation of crystallite size by different energy pulses (200, 300, 400, 500 and 600) mJ, respectively.

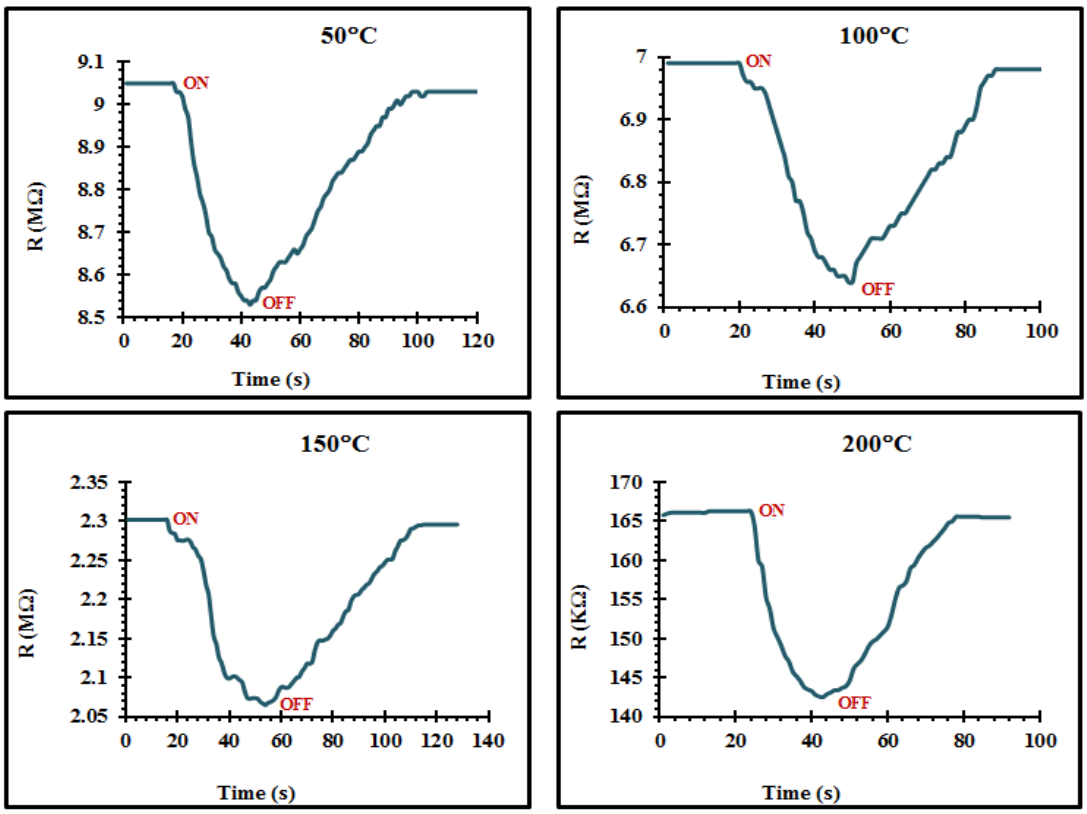

(a)

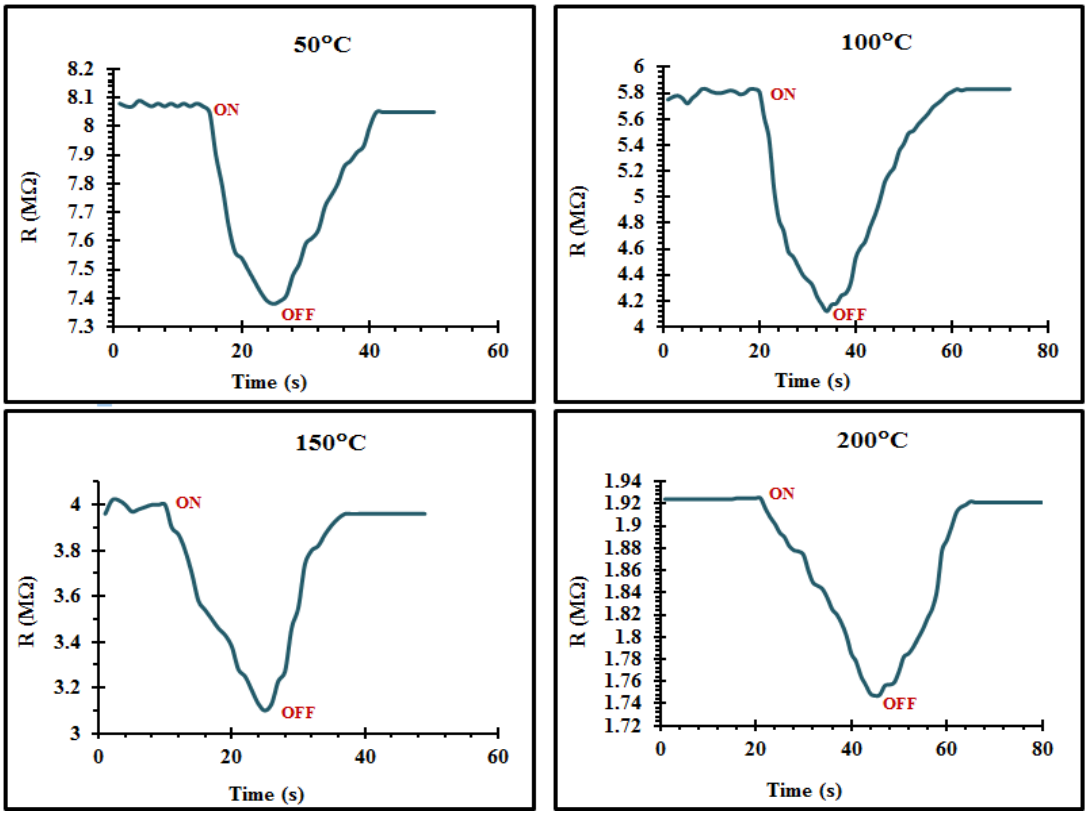

(b)

Fig. 7: The variation of resistance as a function to the time with variation of crystallite size (a): 17.5 nm, (b): 20.6 nm.

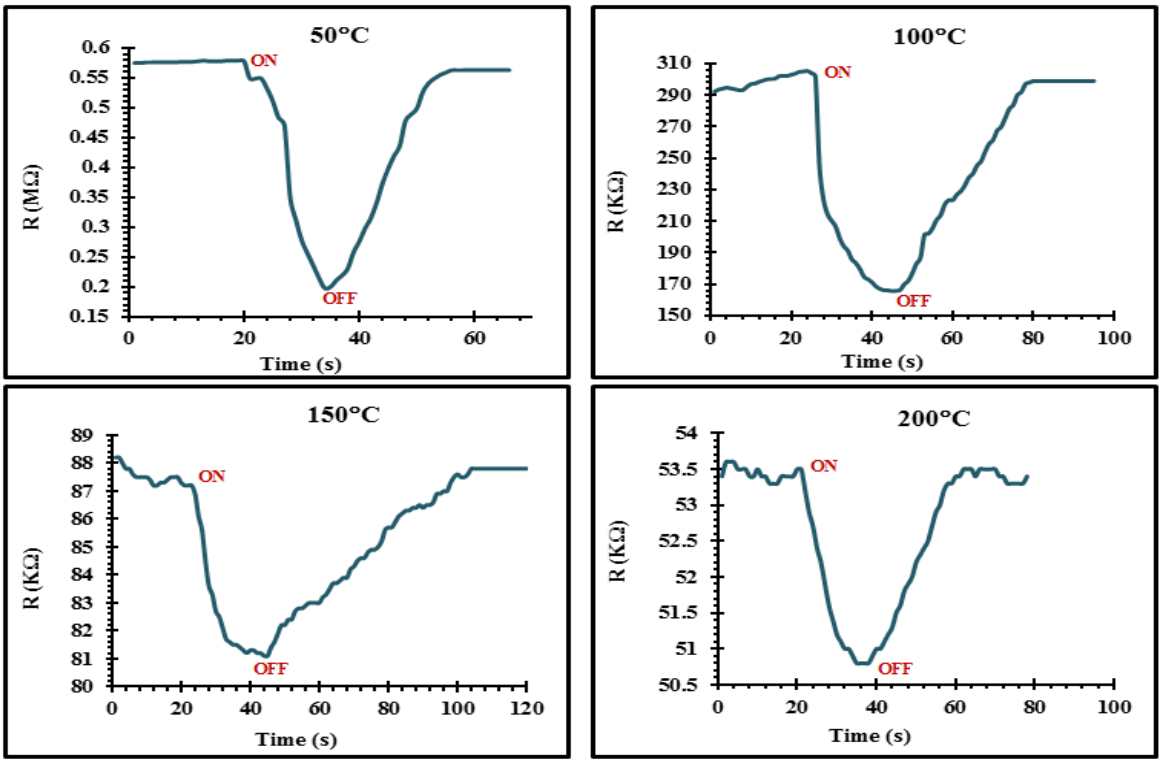

(c)

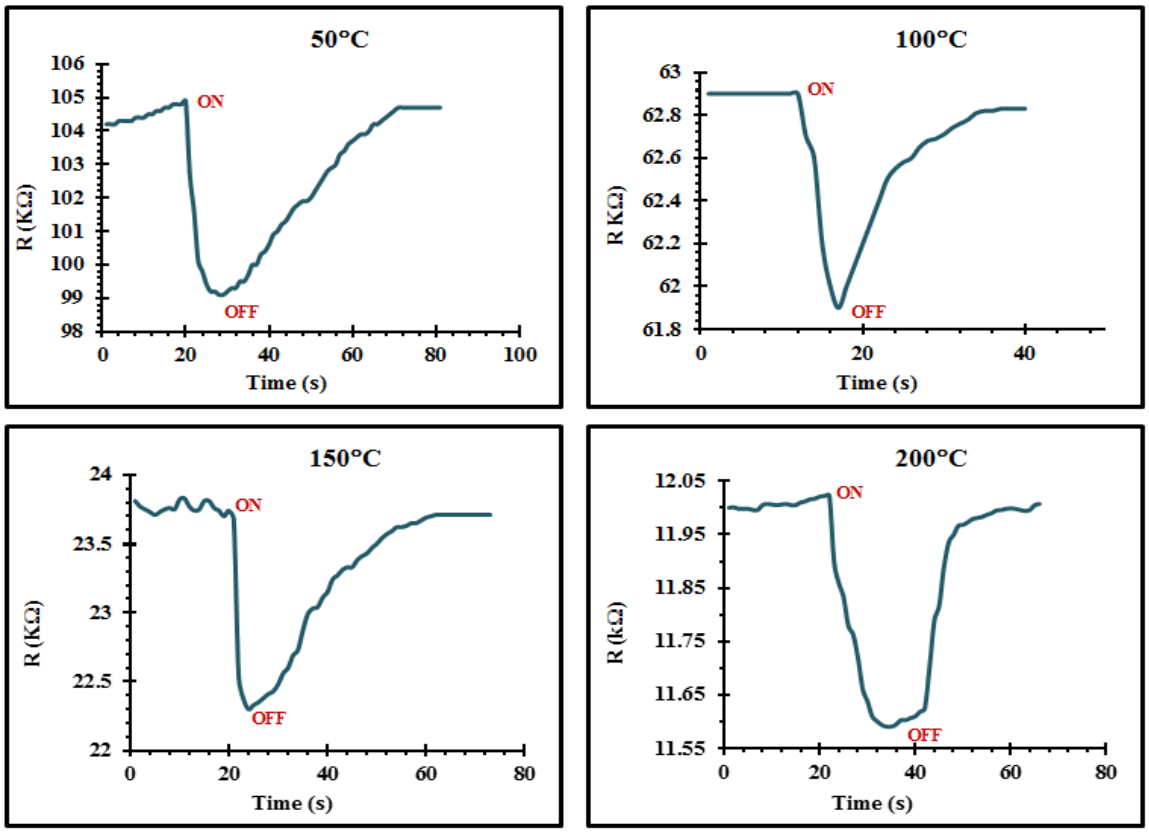

(d)

Fig. 7: The variation of resistance as a function to the time with variation of crystallite size (c): 26.8 nm, (d): 29.3 nm.

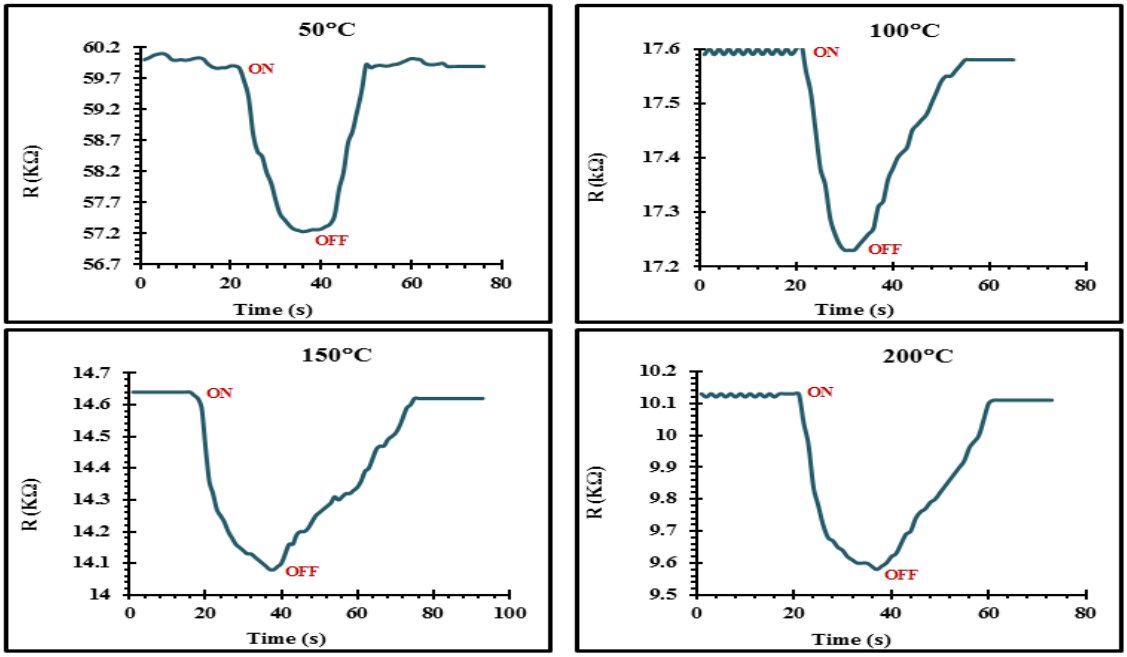

(e)

Fig. 7: The variation of resistance as a function to the time with variation of crystallite size (e): 34.9 nm.

The sensing mechanism of CuO is related to the ionosorption of gas species over the surface, leading to charge transfer between the gas and surface molecules and changes in the electrical conductance [20]. igures show decreasing in the resistance value when their films exposure to NO_2 gas then the resistance value increasing upward at the closure of the gas. This result can be explained as follow; the target gas interacts with the surface of the metal oxide film (generally through surface adsorbed oxygen ions), which results in a change in charge carrier concentration of the material. This change in charge carrier concentration serves to alter the conductivity (or resistivity) of the material.

Fig.7 shows that the resistance decreased in open the gas case and then rapidly increasing in close gas case which denoted to a p-type carrier concentration, where a p-type semiconductor is a material that conducts with positive holes charge carriers; hence, an increase in conductivity in the presence of an oxidising gas [21, 22], because NO_2 is oxiding gas and when applied on a p-type surface film adsorbed to oxygen ions at the grain boundaries and the charge carrier concentration will decrease so the conductivity will decrease, this results is in agreement with (A. Z. Sadek et al.) [23].

Determination of operation temperature of sensor

The operating temperature is defined as the temperature at which the resistance of the sensor reaches a constant value. the changing of resistance is just only influenced by the presence of amount of some gases of interest [24]. The sensitivity factor (S%) at various operating temperatures is calculated using equation: [23, 25]

$$S = \left|\frac{(R_g - R_a)}{R_a}\right| \times 100\% \qquad (5)$$

where: S is the sensitivity, R_a and R_g are the electrical resistance of the film in the air and electrical resistance of

the film in the presence of gas, respectively.

Fig.8 shows the sensitivity as a function of operating temperature CuO films with variation of crystallite size. The gas sensitivity tests were performed at RT, 100°C, 150°C and 200°C. There is an increase and decrease in the sensitivity which indicates the adsorption and desorption phenomenon of the gas. The higher sensitivity may be due to the largest surface area, larger rate of oxidation and the optimum surface roughness. The maximum sensitivity to NO_2 gas was observed to the sample of laser pulses energy with crystallite size of 26.8nm and found to be 91% at RT.

The response time of a gas sensor is defined as the time it takes the sensor to reach 90% of maximum/minimum value of conductance upon introduction of the reducing/oxidizing gas. Similarly, the recovery time is defined as the time required to recover to within 10% of the original baseline when the flow of reducing or oxidizing gas is removed [26].

Fig.9 shows the relation between response and recovery time at optimum operating temperature as a function to the crystallite size of CuO films for NO_2 gas sensing. The response speed is studied at the temperature at which the sensor exhibited a maximum sensitivity. It shows that the sample of laser pulses energy with 26.8nm crystallite size exhibits a fast response speed (7 seconds) with recovery time (44 seconds). The quick response sensor for NO_2 gas may be due to faster oxidation of gas, and in real situations a fast response time is usually required, but a fast recovery time is not so important in sensing measurement [27].

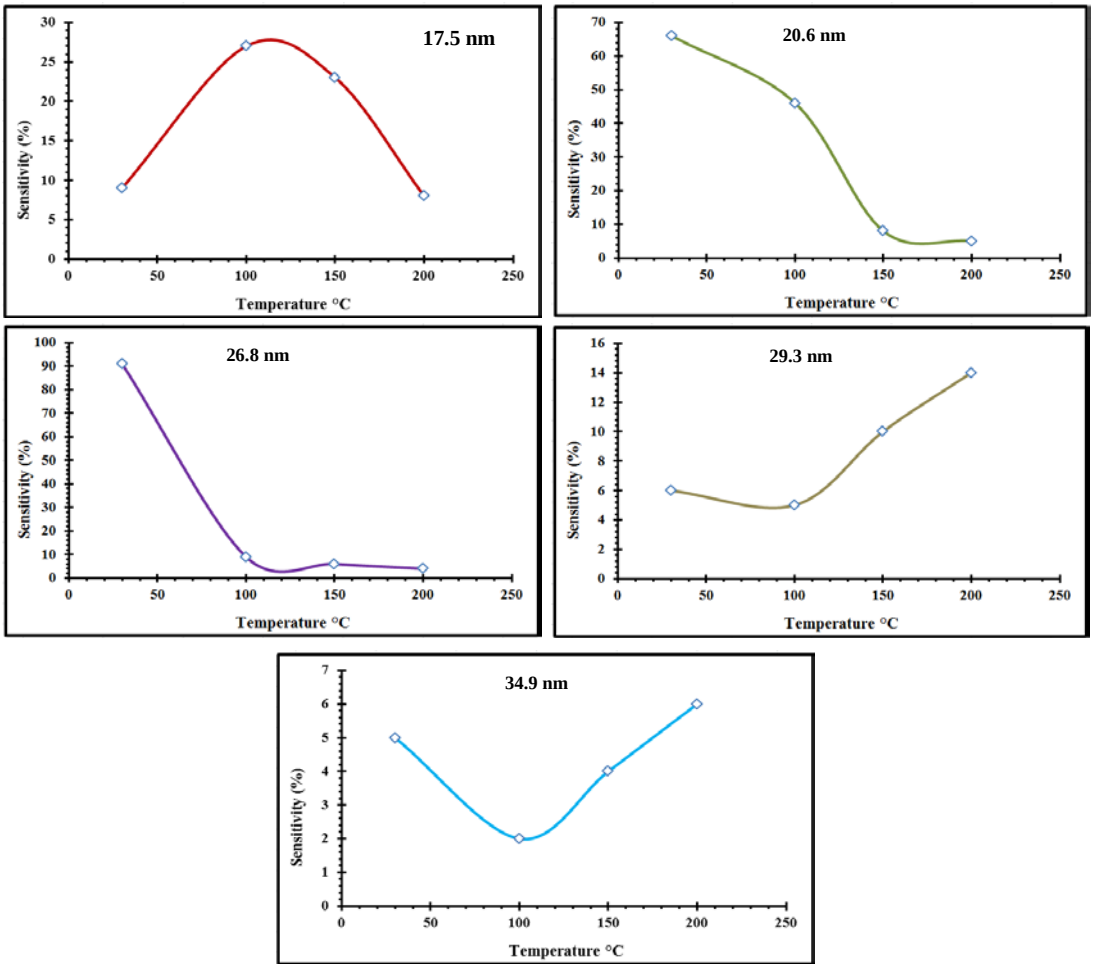

Fig. 8: The variation of NO_2 sensitivity with the operating temperature of CuO films.

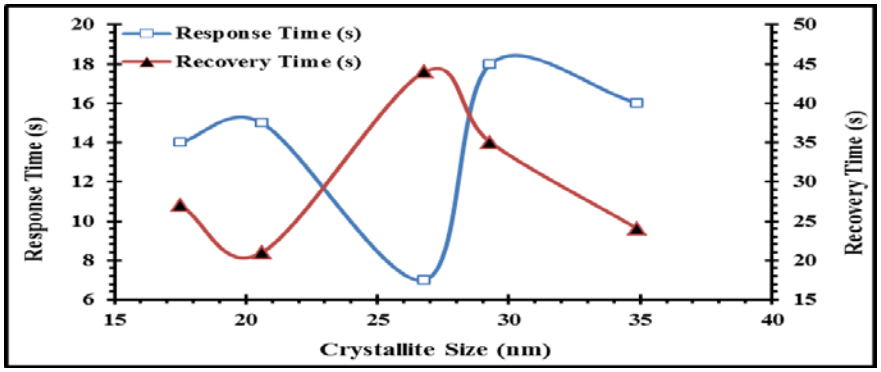

Fig. 9: Response and recovery time as a function to the laser pulses energy.

Conclusion

Cupric oxide thin films were prepared successfully by (PLD) technique. Structural analysis showed a polycrystalline structure with a monoclinic symmetry and preferred orientation toward (111) plane. Increasing in the crystallite size with increasing of laser pulse energy. Optical properties showed increasing in transmittance of all films with increasing in the incident laser pulse energy. Optical energy gap variety from 2.2 to 1.95 eV with increasing in crystallite size. Gas sensing measurement for NO_2 gas revealed that the sample of laser pulses energy 26.8nm crystallite size exhibits a fast response speed (7 seconds) with recovery time of (44 seconds) with sensitivity of 91% at room temperature (50°C).

Reference

[1] K. L. Chopra, S. Major, D. K. Pandya, Thin Solid Films, 102, 1 (1983) 1–46.
[2] V. T. Nguyen, Int. Sch. Res. Not., 2014, 10 (2014) 1–14.
[3] P. Kuprik, O. Filem, S. Kaca, Sains Malaysiana, 43, 4 (2014) 617–621.
[4] D. Barreca, E. Comini, A. Gasparotto, C. Maccato, C. Sada, G. Sberveglieri, E. Tondello, SNB Sensors Actuators B. Chem., 141, 1 (2009) 270–275.
[5] N. Yamazoe, Sensors Actuators, B Chem, 108 (2005) 2–14.
[6] N. B. and U. Weimar, J. Electroceramics, 7 (2001) 143–167.
[7] N. B. and U. W. S. Pokhrel, C. E. Simion, V. Quemener, Sensors Actuators, B Chem, 133 (2008) 78–83.
[8] J. Morales, L. Sánchez, F. Martín, J. R. Ramos-Barrado, M. Sánchez, Thin Solid Films, 474, 1–2 (2005) 133–140.
[9] Y. R. Hathal, I. M. Ibrahim, F. T. Ibrahim, M. H. Ali, Aust. J. Basic Appl. Sci., 9 (2015) 682–688.
[10] T. Maruyama, Sol. Energy Mater. Sol. Cells, 56, 1 (1998) 85–92.
[11] N. Nafarizal, Int. Conf. Semicond. Electron. Proceedings, ICSE, (2014) 100–103.
[12] N. A. M. Shanid and M. A. Khadar, Thin Solid Film., 516, 18 (2008) 6245–6252.
[13] A. A. Ogwu, E. Bouquerel, O. Ademosu, S. Moh, E. Crossan, F. Placido, J. Phys. D. Appl. Phys., 38, 2 (2005) 266–271.
[14] A. S., A. N., R. H.A., R. M., AIP Conf. Proc, 1217 (2010) 37–41.
[15] G. Li, X. Zhu, X. Tang, W. Song, Z. Yang, J. Dai, Y. Sun, X. Pan, S. Dai, J. Alloy. Compd.m 509, 14 (2011) 4816–4823.
[16] A. E. a Said, M. M. A. El-wahab, S. a Soliman, M. N. Goda, Nanosci. Nanoeng., 2, 3 (2014) 17–28.
[17] J. I. Pankove, Optical processes in semiconductors. Englewood Cliffs, (1971), Prentice-Hall.

[18] Sze, S.M, Physics of semiconductor devices., J. wiley and Sons (1981) ^{2}nd Edition.
[19] K.A. Aadim, A.A. Hussain, M.R. Abdulameer, Acta Phys Pol., 128, 3 (2015) 419–422.
[20] L. Filipovic, S. Selberherr, G. C. Mutinati, E. Brunet, S. Steinhauer, K. Anton, J. Teva, J. Kraft, F. Schrank, C. Gspan, W. Grogger, Eng. Lett., 21, 4 (2013) 224–240.
[21] N. Barsan, M. Schweizer-Berberich, W. Gpel, Fresenius J. Anal Chem Fresenius, 365, 4 (1999) 287–304.
[22] D. E. Williams, Sensors Actuators B, 57, 1 (1999) 1–16.
[23] A. Z. Sadek, W. Wlodarski, K. Kalantar-Zadeh, and S. Choopun, Proc. IEEE Sensors, 2005, 2 (2005) 1326–1329.
[24] T. Sujitno S. Sudjatmoko, "T," Atom Indo. Atom Indones., 32, 2 (2011) 503–514.
[25] P. L.A., B. A.R., S. M.D., D. V.V., A. D.P., IEEE Sensors J., 11, 4 (2011) 939–946.
[26] S. VV, B. BK, K. Wepsiec, S. Dmitriev, A. Kolmakov, Nano Lett., 6, 8 (2006) 1584–1588.
[27] S. A. Garde, Sensors Transducers J., 122, 11 (2010) 128–142.
[28] Drift, A. van der. A. van der Drift, Philips Res, 22, (1967) 267.